

# Broad-Band X-Ray Study of a Transient Pulsar RX J0059.2–7138

Makoto KOHNO, Jun YOKOGAWA, and Katsuji KOYAMA\*

*Department of Physics, Graduate School of Science, Kyoto University, Sakyo-ku, Kyoto 606-8502**E-mail(MK): kohno@cr.scphys.kyoto-u.ac.jp*

(Received 1999 August 31; accepted 1999 December 15)

## Abstract

We report on the results of the ASCA and ROSAT observations on RX J0059.2–7138, a transient X-ray pulsar in the Small Magellanic Cloud. The barycentric pulse period has been precisely determined to be  $2.763221 \pm 0.000004$  s. The pulse shape is almost identical in all of the energy bands. The pulse fraction increases with the photon energy below  $\sim 2$  keV, while it is nearly constant at  $\sim 37\%$  above  $\sim 2$  keV. The X-ray spectrum has been found to consist of two components. One is dominant above 2 keV, and exhibits sinusoidal pulsations. This component is well described by a typical model found in many X-ray binary pulsars, a power-law of photon index 0.4 with an exponential cut-off at 6.5 keV. The other is dominant below 1 keV and shows no significant pulsation. This component is represented by either a broken power-law with photon indices of 2.6 and 5.1 below and above a break energy of 0.9 keV, or a metal-poor thin-thermal plasma with a temperature of 0.37 keV. The phase-averaged luminosity is  $\sim 10^{38}$  erg s $^{-1}$  (0.1–10.0 keV) for both components. A hint of oxygen over-abundance is found in the absorbing column, possibly due to circumstellar gas ejected from an evolved companion.

**Key words:** circumstellar matter — pulsars: individual (RX J0059.2–7138) — stars: Be — stars: neutron — X-rays: binaries

## 1. Introduction

Accretion-powered X-ray pulsars are binary systems consisting of a neutron star and a stellar companion (here, X-ray binary pulsars or XBPs in short). The gravitational energy of accreting matter is converted to X-ray radiation, hence its luminosity is generally variable, depending on the mass-accretion rate. Transient behavior is also observed from many XBPs, most of which have a Be star companion with an eccentric orbit (e.g. Stella et al. 1982; Bildsten et al. 1997).

XBPs have been observed mainly in the hard X-ray band ( $\sim 2$ –40 keV) with non-imaging satellites (e.g. Nagase 1989). Their spectra are generally described by a power-law with a high-energy exponential cut-off (hereafter, ECUT power-law) with a photon index of  $\Gamma \sim 1$  and a cut-off energy at around 10–20 keV. A fluorescent emission line at 6.4 keV from neutral iron atoms has been observed in many bright XBPs, which serves as a probe of the circumstellar matter of the binary system. In the soft X-ray band (below  $\sim 2$  keV), however, their spectra have not been well studied due to a large interstellar absorption, because most of the XBPs are located in the galactic plane (e.g. Bildsten et al. 1997).

In order to study soft X-rays from XBPs, therefore, the

Magellanic Cloud sources have great advantages, owing to the low interstellar absorption and well-calibrated distances. Woo et al. (1995, 1996) made broad-band spectroscopic studies in the 0.1–40 keV band of SMC X-1 and LMC X-4, respectively, and found a “soft excess” below  $\sim 2$  keV, in addition to the usual hard spectrum given by an ECUT power-law model. Such a soft excess was also discovered from a transient XBP XTE J0111.2–7317 in the Small Magellanic Cloud (SMC), by an ASCA observation in the 0.5–10.0 keV band (Yokogawa et al. 2000). However, since such a broad-band spectroscopy has been performed on only a few XBPs, whether or not the soft component is common among XBPs is still unclear, especially for transient XBPs.

Hughes (1994) serendipitously discovered a new transient XBP, RX J0059.2–7138, in the SMC with the soft X-ray band observation of ROSAT, and found that the spectrum is unusually soft, which is composed of a blackbody with a temperature of  $kT \sim 35$  eV and a steep power-law with a photon index of  $\Gamma \sim 2.4$ . A proposed candidate for the optical counterpart was revealed to be a Be star by Southwell and Charles (1996).

In order to examine the nature of the unusually soft spectrum of RX J0059.2–7138, observations in the higher energy band are essential. RX J0059.2–7138 was also detected in a simultaneous observation of the SNR E 0102–72.2 with the ASCA satellite, which is sensitive

\* CREST, Japan Science and Technology Corporation (JST), 4-1-8 Honmachi, Kawaguchi, Saitama 332-0012.

in the  $\sim 0.7\text{--}10.0$  keV band. A preliminary short report on the ASCA results can be found in Kylafis (1996).

In this paper, we combine the ROSAT and ASCA data, and perform a broad-band timing spectroscopy, covering  $\sim 0.1\text{--}10.0$  keV. We show that the spectrum of RX J0059.2–7138 has a hard component, which resembles the spectra of usual XBPs well, and that the pulsations are due to the hard component. In addition, a non-pulsating soft component is present in the spectrum. We assume the distance to RX J0059.2–7138 to be 60 kpc, the nominal value to the SMC (Mathewson 1985).

## 2. Observations

The transient XBP RX J0059.2–7138 was serendipitously detected on May 12–13 in 1993, in the simultaneous ASCA and ROSAT observations of E 0102–72.2, the brightest supernova remnant in the SMC. ASCA and ROSAT observations spanned about 99 ks (MJD 49119.38–MJD 49120.52) and 20 ks (MJD 49119.95–MJD 49120.18), respectively.

ASCA carries four X-ray Telescopes (XRT) with two Gas Imaging Spectrometers (GIS 2 and GIS 3) and two Solid-state Imaging Spectrometers (SIS 0 and SIS 1) on the focal planes (Tanaka et al. 1994; Serlemitsos et al. 1995; Ohashi et al. 1996; Burke et al. 1994). Since RX J0059.2–7138 was outside of the SISs' field of view and was located near the calibration source of GIS 3, we used only the GIS 2 data in this paper. The GISs were operated in the normal PH mode with a time resolution of 0.0625 s (high bit rate) or 0.5 s (medium bit rate). We rejected any data obtained when the satellite was in the SAA (South Atlantic Anomaly) region, when the elevation angle of the Earth limb was less than  $5^\circ$  or when the cut-off rigidity was less than 4 GV, and also removed particle events using the rise-time discrimination method. The total exposure time of GIS 2 was  $\sim 35$  ks after screening.

ROSAT carries a soft X-ray telescope with a High Resolution Imager (HRI) and a Position Sensitive Proportional Counter (PSPC) with one of the two on the focal plane (Trümper 1983). In this observation, PSPC-B was on the focus and operated in the pointing mode. We took the screened data from the HEASARC archive, of which the total exposure time was  $\sim 5$  ks.

## 3. Analyses and Results

For the GIS data, X-ray photons were collected from an elliptical region around RX J0059.2–7138 (figure 1). The background data were extracted from off-source areas on the edge of GIS 2 at the same off-axis angle as the source (figure 1), because both the diffuse X-rays and non-X-ray background depend on the off-axis angle.

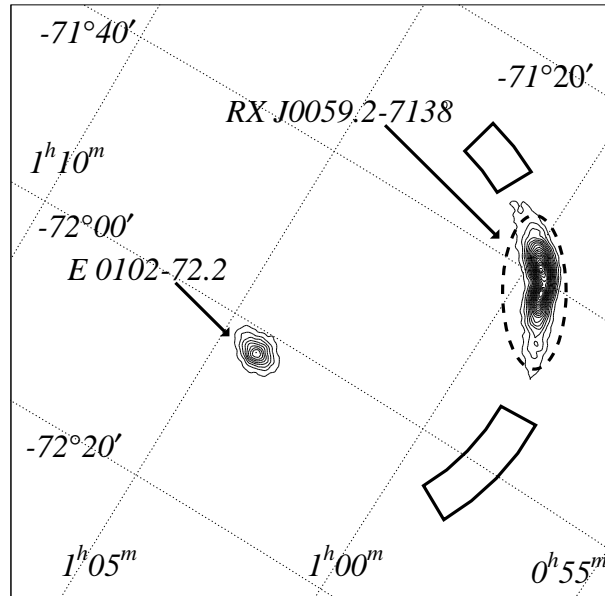


Fig. 1.. ASCA GIS 2 image. The sources detected at the center and the edge are the SNR E 0102–72.2 and RX J0059.2–7138, respectively. The photons of RX J0059.2–7138 were spreaded by the point-spread function at the detector edge region. The source and background regions used in the analyses are enclosed by the dashed and solid lines, respectively.

As for the ROSAT PSPC, we selected a circular region of  $3'$ -radius around the source, while the data from an annulus of inner and outer radii  $3'$  and  $6'$  were used as the background. Since a super-soft source (SSS) 1E 0056.8–7154 was located at  $4'$  northwest of RX J0059.2–7138 and the X-ray flux of this SSS was fairly large in the ROSAT band below  $\sim 0.5$  keV, we excluded a circular region of a  $3'$ -radius around this SSS from the analyses of the ROSAT PSPC.

### 3.1. Timing Analysis

In total, the numbers of counts from the source regions are 21847 in the  $0.7\text{--}10.0$  keV band (ASCA GIS 2) and 23250 in the  $0.07\text{--}2.4$  keV band (ROSAT PSPC). After the barycentric correction of arrival time for each event, we carried out timing analyses.

The pulse period was already determined to be  $2.7632 \pm 0.0002$  s with the ROSAT data alone (Hughes 1994). We used the ASCA data to obtain a more precise period, because the duration of the ASCA observation is nearly five-times longer than the ROSAT observation. We performed epoch-folding on all of the ASCA GIS 2 data, and determined a trial pulse period to be 2.76322 s. We then divided the ASCA observation into three segments, each having a duration of  $\sim 33$  ks, and folded each of the light curves with a trial period of 2.76322 s.

To the folded pulse profiles of the first and the last segments, we made a cross correlation, and determined

the average apparent barycentric pulse period during the observation to be  $2.763221 \pm 0.000004$  s. This value is consistent with, and more precise than, the previous result of  $2.7632 \pm 0.0002$  s (Hughes 1994).

The cross correlation between the middle and the first/last segments shows the upper limit of the phase difference to be  $\sim 0.04$ . Based on the assumption of a constant period change during the observation, this upper limit of the phase difference is converted to the upper limit of the period derivative of  $|\dot{p}| < 6 \times 10^{-10}$  s s $^{-1}$ .

Figure 2 shows the pulse profiles in the six energy bands (0.07–0.4 keV, 0.4–1.0 keV, and 1.0–2.4 keV in ROSAT PSPC, and 0.7–2.0 keV, 2.0–4.0 keV, and 4.0–10.0 keV in ASCA GIS) folded with a pulse period of 2.763221 s. The pulse fractions, defined as  $(I_{\max} - I_{\min})/2I_{\text{average}}$ , in these energy bands are  $0.07 \pm 0.06$ ,  $0.14 \pm 0.04$ ,  $0.26 \pm 0.04$  (0.07–0.4 keV, 0.4–1.0 keV, and 1.0–2.4 keV in ROSAT PSPC) and  $0.24 \pm 0.05$ ,  $0.37 \pm 0.05$ , and  $0.36 \pm 0.05$  (0.7–2.0 keV, 2.0–4.0 keV, and 4.0–10.0 keV in ASCA GIS), respectively. The pulse shape is nearly sinusoidal and independent of the X-ray energy. The apparent decrease of the pulse fraction with decreasing energy, which was already found in the ROSAT data (Hughes 1994), is also seen in the ASCA data below  $\sim 2$  keV.

On a longer timescale (50–100 s), Hughes (1994) reported a flickering variability of about 30% of the mean rate in the ROSAT data. Such variability was also seen in the ASCA data with no energy dependence, while no larger variability, like a burst, was detected.

### 3.2. Spectral Analysis

Figure 3 shows the phase-averaged spectra after background subtraction. Since the pulse profile is essentially energy independent while the pulse fraction increases with energy below  $\sim 2$  keV, we can naturally assume that the spectrum of RX J0059.2–7138 consists of two components: a hard component dominant above  $\sim 2$  keV, which has an energy-independent pulsation, and a soft component dominant below  $\sim 2$  keV with no pulsation.

With this working hypothesis, we first determined the hard component using the ASCA spectrum above  $\sim 2$  keV. Since no significant emission line was detected, we fitted the spectrum with a single power-law model. However, because systematic negative residuals remained above  $\sim 7$  keV, we introduced a high-energy exponential cut-off to the single power-law model (ECUT power-law) and fitted the spectrum again. We then obtained an acceptable fit to an ECUT power-law model with a photon index of  $\Gamma \sim 0.4$ , a cut-off energy of  $E_c \sim 6.6$  keV and a folding energy of  $E_f \sim 8.8$  keV.

To investigate the soft component, we then simultaneously fitted the ROSAT and ASCA spectra in the 0.1–10.0 keV band with various two-component mod-

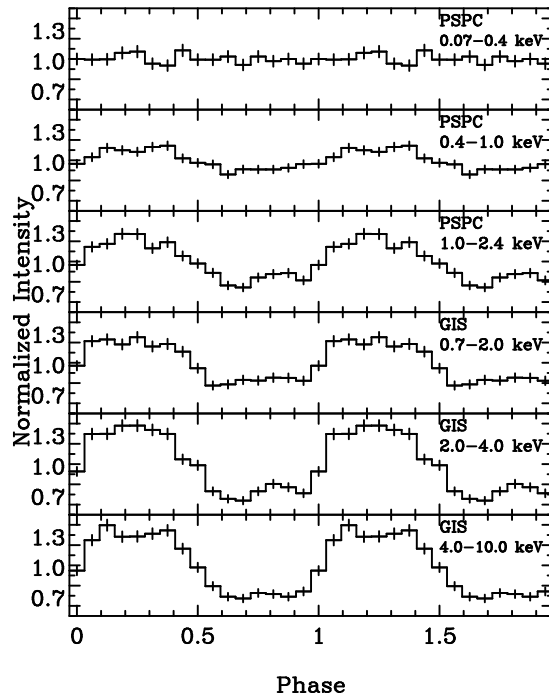


Fig. 2.. Normalized intensities of the folded light curves. The background levels are  $\sim 1\%$  and  $\sim 10\%$  of the average, in the PSPC data and in the GIS 2 data, respectively.

els, in which an ECUT power-law model was always adopted to the hard component. For the additional soft component, we adopted a blackbody, disk blackbody, bremsstrahlung, thin-thermal plasma (Mewe et al. 1985), and broken power-law model. In these two-component model fits, a common absorbing gas column with solar abundance was adopted for both the hard and soft components. All models were statistically rejected at the 90% confidence level with wavy residuals below  $\sim 1$  keV. In particular, an edge-like structure was seen at  $\sim 0.5$  keV, which may correspond to the absorption edge of neutral oxygen atoms. Allowing the oxygen abundance in the absorption column to be free, we obtained statistically acceptable fits only when the soft component was either a thin-thermal plasma or a broken power-law. The best-fit parameters for these models are separately listed in tables 1 and 2, while the best-fit model is shown in figure 3.

We separately made phase-resolved spectra from phases 0–0.5 (‘on-pulse’) and 0.5–1 (‘off-pulse’). We fit these spectra with the two accepted models, and found that only the normalization of the hard component varies with the pulse phase. The best-fit parameters of these models are also listed in tables 1 and 2, while the best-

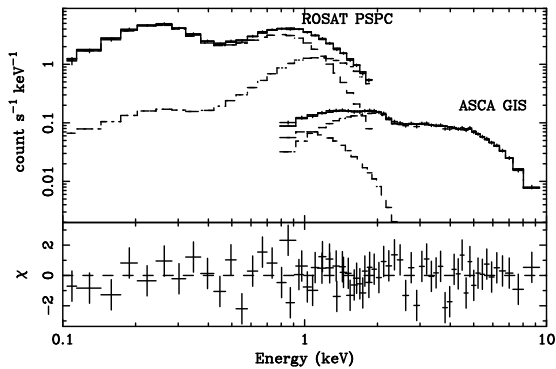


Fig. 3.. Phase-averaged spectra. (Upper panel): Data are shown by crosses. The best-fit model (a thin-thermal plasma plus an ECUT power-law) of ROSAT PSPC and ASCA GIS are plotted with lines. (Lower panel): Residuals from the best-fit model.

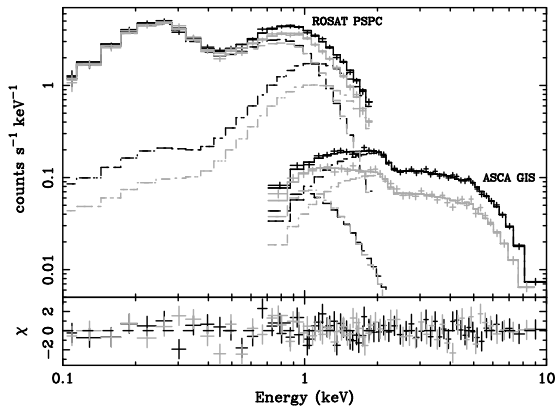


Fig. 4.. Phase-resolved spectra. (Upper panel): Data are shown by crosses. The best-fit model (a thin-thermal plasma plus an ECUT power-law) of ‘on-pulse’ and ‘off-pulse’ are plotted with black and gray lines, respectively. (Lower panel): Residuals from the best-fit model.

fit model is shown in figure 4. We also extracted the “pulsed spectrum” by subtracting the off-pulse spectrum from that of on-pulse. We found that the pulsed spectrum is fitted with an ECUT power-law with absorption, of which the best-fit parameters are consistent with those of the hard component of the phase-averaged spectrum. These facts indicate that the pulsating X-rays contribute only to the hard component, consistent with the initial working hypothesis.

## 4. Discussion

### 4.1. Comparison to the Previous Results

Hughes (1994) analyzed only the ROSAT data, and showed that the spectrum is fitted by a model having

an extremely soft spectrum: a blackbody ( $kT \sim 35$  eV) plus a steep power-law ( $\Gamma \sim 2.4$ ). However, we have shown that the spectrum in the ASCA band (the hard component) is as hard as those of usual XBPs, and the ROSAT spectrum consists of mostly the “soft excess” below  $\sim 2$  keV.

For a consistency check, we first fitted our ROSAT spectrum with Hughes’ model, and obtained best-fit parameters consistent with Hughes (1994). However, as can be also seen in figure 2 in Hughes (1994), systematic positive residuals were found above  $\sim 1.5$  keV, which implies the existence of a hard component. We then fitted the ASCA and ROSAT spectra simultaneously with a three-component model, consisting of the hard ECUT power-law to the Hughes’ two-component model. In this model, the best-fit blackbody temperature became much lower than the original result. After corrections for absorption and detector efficiency, the bolometric luminosity of the soft black body has an unrealistic value of  $\sim 10^{45}$  erg  $s^{-1}$ .

On the other hand, as we found, the combined ASCA and ROSAT spectra can be fitted with two different components, with a more reasonable luminosity of  $\sim 10^{38}$  erg  $s^{-1}$  for both components. Also, the energy-dependent pulse fraction and energy-independent pulse profile are naturally explained by our two-component model. We thus infer that the present model is more probable, hence the spectrum of RX J0059.2–7138 is not unusual for an XBP, at least in the hard energy band.

### 4.2. Oxygen Over-Abundance

We found an edge-like structure at 0.5 keV, which would be a hint of over-abundance of oxygen in the absorbing matter. One may argue, however, that the ROSAT spectrum fitted by Hughes (1994) does not show any structure at 0.5 keV. We should note that the blackbody and power-law components in the Hughes’s model cross at around 0.5 keV, which may produce an artificial dip, and hence would compensate for the edge-like structure.

To check whether the structure is real or not, we fitted a narrow-band spectrum (0.2–0.8 keV) with a power-law absorbed by cool matter of solar abundance. Because the structure remained near 0.5 keV, we claim that the edge-like structure is real.

Since the oxygen abundance of the SMC interstellar matter is less than the solar value (Russell, Dopita 1992), we can infer that there exists oxygen-rich matter around the binary system of RX J0059.2–7138. The companion star, which should have ejected the oxygen-rich matter, may be in an evolved stage where the stellar surface becomes abundant only in oxygen, although such stars (e.g. WO stars) are very rare.

On the other hand, metals such as carbon, nitrogen, and oxygen could be brought to the surface of a massive

Table 1. Best-fit parameters for a thin-thermal plasma plus an ECUT power-law model.

	$kT$ (keV)	$Z^*$ ( $10^{-2}$ solar)	$\Gamma$	$E_c$ (keV)	$E_f$ (keV)	$N_H^\dagger$ ( $10^{20}$ cm $^{-2}$ )	$Z_O^\ddagger$ (solar)	$L_{xs}^\S$ ( $10^{38}$ erg s $^{-1}$ )	$L_{xh}^\S$	$\chi^2/\text{d.o.f.}$
Av.	$0.37^{+0.02}_{-0.04}$	$1.5^{+0.8}_{-0.6}$	$0.43^{+0.05}_{-0.05}$	$6.4^{+0.8}_{-0.9}$	$9.3^{+11.2}_{-4.3}$	$4.2^{+0.2}_{-0.2}$	$7.3^{+1.9}_{-1.8}$	0.8	1.8	63.9/62
On	$0.35^{+0.04}_{-0.03}$	$1.6^{+1.4}_{-0.9}$	$0.48^{+0.06}_{-0.07}$	$6.5^{+1.1}_{-1.1}$	$8.5^{+11.7}_{-4.5}$	$4.3^{+0.3}_{-0.3}$	$6.4^{+2.8}_{-2.4}$	0.8	2.2	48.6/62
Off	$0.38^{+0.03}_{-0.04}$	$1.6^{+1.4}_{-0.8}$	$0.47^{+0.10}_{-0.10}$	$5.9^{+1.3}_{-1.0}$	$8.3^{+16.3}_{-5.1}$	$4.0^{+0.3}_{-0.3}$	$8.7^{+3.2}_{-2.5}$	0.8	1.2	59.4/59

Note—The errors are at the 90% confidence level.

\*: Metal abundance of the thin-thermal plasma in unit of 1% of the solar abundance.

†: Absorption column density with the solar abundance (except oxygen) in unit of  $10^{20}$  H cm $^{-2}$ .

‡: Oxygen abundance in the absorbing matter in unit of the solar abundance.

§: Absorption corrected luminosities of the soft and hard components in the 0.1–10.0 keV band at a distance of 60 kpc, in unit of  $10^{38}$  erg s $^{-1}$ .

Table 2. Best-fit parameters for a broken power-law plus an ECUT power-law model.

	$\Gamma_1^*$	$\Gamma_1'$	$E_{b1}^*$ (keV)	$\Gamma_2$	$E_c$ (keV)	$E_f$ (keV)	$N_H^\dagger$ ( $10^{20}$ cm $^{-2}$ )	$Z_O^\ddagger$ (solar)	$L_{xs}^\S$ ( $10^{38}$ erg s $^{-1}$ )	$L_{xh}^\S$	$\chi^2/\text{d.o.f.}$
Av.	$2.6^{+0.3}_{-0.7}$	$5.1^{+0.9}_{-0.6}$	$0.9^{+0.1}_{-0.1}$	$0.41^{+0.06}_{-0.07}$	$6.4^{+0.6}_{-0.9}$	$9.0^{+14.0}_{-4.0}$	$5.0^{+0.6}_{-1.2}$	$4.3^{+2.5}_{-1.6}$	0.8	1.8	63.0/61
On	$2.5^{+0.5}_{-1.5}$	$5.3^{+3.3}_{-0.9}$	$0.9^{+0.2}_{-0.1}$	$0.46^{+0.07}_{-0.08}$	$6.5^{+1.0}_{-1.1}$	$8.4^{+11.1}_{-4.4}$	$4.9^{+1.1}_{-2.6}$	$4.3^{+4.9}_{-2.9}$	0.9	2.2	48.7/61
Off	$2.6^{+0.4}_{-0.7}$	$5.2^{+1.8}_{-0.8}$	$0.9^{+0.2}_{-0.1}$	$0.46^{+0.12}_{-0.16}$	$5.9^{+1.3}_{-1.0}$	$8.1^{+16.8}_{-4.9}$	$5.0^{+0.7}_{-1.4}$	$4.5^{+2.1}_{-1.9}$	1.1	1.3	57.4/58

Note—The errors are at 90% confidence level.

\*:  $\Gamma$  and  $\Gamma'$  are photon indices below and above  $E_b$ , respectively.

†: Absorption column density with the solar abundance (except oxygen) in unit of  $10^{20}$  H cm $^{-2}$ .

‡: Oxygen abundance of the absorbing matter in unit of the solar abundance.

§: Absorption corrected luminosities of the soft and hard components in the 0.1–10.0 keV band at a distance of 60 kpc, in unit of  $10^{38}$  erg s $^{-1}$ .

star by turbulent diffusion, due to the rapid rotation or tides in a binary system (Maeder 1987). We thus fitted the spectra again, based on the assumption that abundances of carbon and nitrogen in the absorbing matter are the same as that of oxygen. The abundance was then determined to be  $\sim 6$  solar, which leads us to a more comfortable possibility that the surface of the companion star is enriched in CNO, which may be caused by tidal effects in the close binary system.

We found that a thin-thermal plasma with very low abundance of 0.02 solar can fit the soft X-ray spectrum. As we discuss in the next subsection, the soft component is likely to originate from a large region surrounding the binary system. This creates a dilemma that the X-ray emitting circumstellar medium is extremely under-abundant, while the X-ray absorbing circumstellar gas is CNO over-abundant. Although we have no clear idea of how to solve this dilemma, we suggest that the thin-thermal plasma is not a physical model, but is a phe-

nomenological model like a broken power-law for the soft component.

#### 4.3. Origin of the Hard and Soft Components

Since the pulsation was found to be mostly due to the hard component, we can conclude that the hard component originates from a small region, probably near to the polar cap of the neutron star. Hence, the origin would be the same as those of other XBPs. However, the cut-off energy is lower than that of the usual XBPs (10–20 keV; e.g. Mihara 1995a). According to the correlation between the cut-off energy and magnetic field strength (Mihara 1995a, 1995b), the magnetic field of RX J0059.2–7138 is estimated to be  $6 \times 10^{11} < B < 1 \times 10^{12}$  G, which is one of the weakest magnetic fields in XBPs.

A puzzle is the origin of the soft component. Since it shows no pulsation, it is likely that the soft component originates from a relatively large region, covering a significant fraction of the full binary system. In

fact, when we adopt the thin-thermal plasma model as the soft component, the emission measure is very large:  $n^2V \sim 10^{61} \text{ cm}^{-3}$  (table 1), where  $n$  and  $V$  are number density and volume of the plasma. If we assume that the plasma is distributed spherically, its radius should be larger than 0.07 AU under the optically thin condition, which does not conflict with the thin thermal scenario for the soft component.

At present, only a few XBPs are known to have a soft excess. Her X-1 has a soft component which is described by a blackbody ( $kT \sim 0.09 \text{ keV}$ ; Dal Fiume et al. 1998), and is pulsating. McCray et al. (1982) found the phase shift between pulse profiles of the soft and the hard components, and argues that the soft component is produced by reprocessing of the hard component in the inner accretion disk. Another XBP, LMC X-4 has a soft component of a blackbody ( $kT \sim 0.03 \text{ keV}$ ) plus a bremsstrahlung ( $kT \sim 0.4 \text{ keV}$ ) (Woo et al. 1996). The blackbody component is almost constant during the pulse phase, while the bremsstrahlung component is pulsating with some phase shift from the hard component. Woo et al. (1996) argued that the blackbody component is emitted from the accretion disk, and the bremsstrahlung component is from somewhere near the neutron star, collimated as a fan-beam.

The soft component of RX J0059.2–7138 is, however, different from these XBPs; it is not pulsating, it is not a blackbody spectrum and it has no emission line. Hence, the origin of the soft X-rays would be different from those proposed by the above-mentioned authors. As a matter of fact, RX J0059.2–7138 is a unique source among the XBPs with soft excess; because it probably has a Be star companion (Southwell, Charles 1996), it is different from either low-mass companion systems (Her X-1) or from high-mass supergiant companion systems (LMC X-4).

Broad-band spectroscopic studies on the spectra of XBPs with a Be star companion have until now been very limited, due to the transient nature of this class and the relatively narrow energy ranges of the previous and contemporaneous satellites. New-generation satellites having a broad-band sensitivity and a wide field of view, such as ASTRO-E, XMM, and Chandra Observatory, will greatly improve our understanding on the soft excess of XBPs.

We express our thanks to J. Hughes, who told us about the serendipitous detection of RX J0059.2–7138 in the GIS field and the referee for his useful comments. J.Y. is supported by JSPS Research Fellowship for Young Scientists. This research has made use of data obtained through the High Energy Astrophysics Science Archive Research Center Online Service, provided by the NASA/Goddard Space Flight Center.

## References

- Bildsten L., Chakrabarty D., Chiu J., Finger M.H., Koh D.T., Nelson R.W., Prince T.A., Rubin B.C. et al. 1997, *ApJS* 113, 367
- Burke B.E., Mountain R.W., Daniels P.J., Dolat V.S., Cooper M.J. 1994, *IEEE Trans. Nucl. Sci.* 41, 375
- Dal Fiume D., Orlandini M., Cusumano G., Del Sordo S., Feroci M., Frontera F., Oosterbroek T., Palazzi E. et al. 1998, *A&A* 329, L41
- Hughes J.P. 1994, *ApJ* 427, L25
- Kylafis N.D. 1996, in *Supersoft X-ray Sources*, ed J. Greiner, *Lecture Notes in Physics* 472 (Springer, Berlin) p41
- Maeder A. 1987, *A&A* 178, 159
- Mathewson D.S. 1985, *Proc. Astron. Soc. Aust.* 6, 104
- McCray R.A., Shull J.M., Boynton P.E., Deeter J.E., Holt S.S., White N.E. 1982, *ApJ* 262, 301
- Mewe R., Gronenschild E.H.B.M., van den Oord G.H.J. 1985, *A&AS* 62, 197
- Mihara T. 1995a, PhD Thesis, The University of Tokyo
- Mihara T. 1995b, *RIKEN Review* No. 10
- Nagase F. 1989, *PASJ* 41, 1
- Ohashi T., Ebisawa K., Fukazawa Y., Hiyoshi K., Horii M., Ikebe Y., Ikeda H., Inoue H. et al. 1996, *PASJ* 48, 157
- Russell S.C., Dopita M.A. 1992, *ApJ* 384, 508
- Serlemitsos P.J., Jalota L., Soong Y., Kunieda H., Tawara Y., Tsusaka Y., Suzuki H., Sakima Y. et al. 1995, *PASJ* 47, 105
- Southwell K.A., Charles P.A. 1996, *MNRAS* 281, L63
- Stella L., White N.E., Rosner R. 1982, *ApJ* 308, 669
- Tanaka Y., Inoue H., Holt S.S. 1994, *PASJ* 46, L37
- Trümper J. 1983, *Adv. Space Sci.* 2, 241
- Woo J.W., Clark G.W., Blondin J.M., Kallman T.R., Nagase F. 1995, *ApJ* 445, 896
- Woo J.W., Clark G.W., Levine A.M., Corbet R.H.D., Nagase F. 1996, *ApJ* 467, 811
- Yokogawa J., Paul B., Ozaki M., Nagase F., Chakrabarty D., Takeshima T. 2000, *ApJ*, submitted